The Astrophysical Journal, 632:1099–1103, 2005 October 20

A STRONG X-RAY BURST FROM THE LOW-MASS X-RAY BINARY EXO 0748−676

Michael T. Wolff
Space Science Division, Naval Research Laboratory, Washington, DC 20375; michael.wolff@nrl.navy.mil

Peter A. Becker
Center for Earth Observing and Space Research, George Mason University, Fairfax, VA 22030-4444; pbecker@gmu.edu

and

Paul S. Ray and Kent S. Wood
Space Science Division, Naval Research Laboratory, Washington, DC 20375; paul.ray@nrl.navy.mil, kent.wood@nrl.navy.mil
Received 2005 March 22; accepted 2005 June 21

ABSTRACT

We have observed an unusually strong X-ray burst as a part of our regular eclipse timing observations of the low-mass binary system EXO 0748−676. The burst peak flux was 5.2×10^{-8} ergs cm^{-2}s^{-1}, approximately 5 times the normal peak X-ray burst flux observed from this source by *RXTE*. Spectral fits to the data strongly suggest that photospheric radius expansion occurred during the burst. In this paper we examine the properties of this X-ray burst, which is the first example of a radius expansion burst from EXO 0748−676 observed by *RXTE*. We find no evidence for coherent burst oscillations. Assuming that the peak burst luminosity is the Eddington luminosity for a 1.4 $M_\odot$ neutron star, we derive a distance to EXO 0748−676 of 7.7 kpc for a helium-dominated burst photosphere and 5.9 kpc for a hydrogen-dominated burst photosphere.

Subject headings: stars: distances — stars: individual (EXO 0748−676) — X-rays: binaries — X-rays: bursts

1. INTRODUCTION

The low-mass X-ray binary (LMXB) system EXO 0748−676 was originally discovered by the *European X-Ray Observatory Satellite* (*EXOSAT*) during 1985 February (Parmar et al. 1985). Observations by *EXOSAT* detected periodic full eclipses and 25 type I X-ray bursts, three of which were reported to show evidence of photospheric radius expansion (Gottwald et al. 1986). EXO 0748−676 was subsequently observed by *GINGA*, *Röntgensattelit* (*ROSAT*), *Advanced Satellite for Cosmology and Astrophysics* (*ASCA*), *BeppoSAX*, *XMM-Newton*, and the *Rossi X-Ray Timing Explorer* (*RXTE*). EXO 0748−676 is a 3.82 hr orbital period system, normally classified as an "atoll" source, with a neutron star primary accreting matter from the Roche lobe-filling, low-mass main-sequence secondary star UY Vol. A possible observation of gravitationally redshifted lines in X-ray burst spectra has been reported by Cottam et al. (2002). Villarreal & Strohmayer (2004) have recently reported a possible spin period for the neutron star of 45 Hz.

EXO 0748−676 is a heavily studied and important LMXB system for investigating accretion physics; thus, constraining its distance as accurately and rigorously as possible is very important. The spectral type of the secondary in EXO 0748−676 has thus far been elusive. An upper limit for the *U*-brightness of the secondary star of 21$^{\rm st}$ magnitude during X-ray quiescence can be estimated based on the absence of detectable emission on the SRC-J survey plate of the EXO 0748−676 region (Wade et al. 1985). Observations of EXO 0748−676 after its discovery by *EXOSAT* during its X-ray active state show an optically erratic variable of near 17$^{\rm th}$ magnitude (van Paradijs et al. 1988). However, van Paradijs et al. attributed the bulk of the optical emission to the neutron star accretion disk. The intrinsic faintness of the secondary and the system location outside the Galactic bulge at $(l,\ b) = (280\overset{\circ}{.}0,\ -19\overset{\circ}{.}8)$ make an accurate reddening distance difficult to obtain (Schoembs & Zoeschinger 1990). Furthermore, its Galactic latitude puts it well out of the Galactic plane, making a Galactic differential rotation distance uncertain by an unknown amount (Crampton et al. 1986). It is also too distant for the present generation of astrometry satellites to measure an accurate parallax. Yet the fact that EXO 0748−676 is a bursting LMXB opens the possibility of obtaining the distance if an Eddington luminosity–limited X-ray burst can be observed and accurately analyzed. Gottwald et al. (1986) analyzed *EXOSAT* observations of three apparent radius expansion bursts but only assumed a distance of 10 kpc to EXO 0748−676 in order to estimate the Eddington luminosity. Jonker & Nelemans (2004) used the Gottwald et al. peak burst flux from the *EXOSAT* Medium Energy detector in order to estimate the distance of EXO 0748−676 to be in the range 6.8–9.1 kpc. Until now, however, no X-ray burst detected by *RXTE* from EXO 0748−676 showing evidence of photospheric radius expansion has been reported.

Since 1996, near the beginning of the *RXTE* mission, we have maintained a program of regular observations of EXO 0748−676, of length 2–3 ks, in order to monitor the eclipses and precisely time the system orbital period (Hertz et al. 1997; Wolff et al. 2002). During our eclipse monitoring observations with the Proportional Counter Array (PCA) on *RXTE*, we serendipitously capture numerous type I X-ray bursts. A typical X-ray burst will rise within seconds to an apparent count rate of roughly 1000 counts s^{-1} PCU^{-1} in the 2–20 keV energy range (∼1/3 crab). However, during 2004 May we observed one X-ray burst that reached a count rate of nearly 5000 counts s^{-1} PCU^{-1} (∼1.7 crab) and showed evidence of photospheric radius expansion. In this paper we report a detailed analysis of this very luminous burst. Assuming the peak burst luminosity is equal to the Eddington luminosity for a 1.4 $M_\odot$ neutron star, we derive a distance to the EXO 0748−676 system of 7.7 kpc for a helium-dominated burst photosphere and 5.9 kpc for a hydrogen-dominated burst photosphere.

2. *RXTE* OBSERVATIONS

During the *RXTE* observation designated by ObsID 90059-03-01-00, we detected a strong X-ray burst that began at MJD (TT;

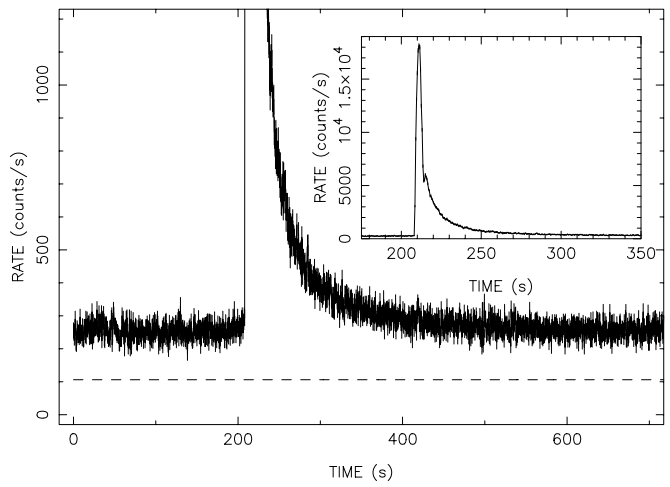

FIG. 1.—Standard-1 light curve of the X-ray burst from the four active PCUs. The dashed line shows the approximate background count level in the PCA during the burst. The preburst light curve shows only a small level of variation consistent with little or no dipping behavior, as noted in the text.

not barycentered) = 53126.40358. Four PCUs (PCU0, PCU1, PCU2, and PCU3) were active during this observation. The observation was done in GoodXenon mode, which preserves full-time and spectral information for each photon event. The burst peak flux saturated the GoodXenon data collection buffer twice during the burst, triggering the burstcatcher mode, which preserves only the event times binned at 122 μs intervals and no spectral (PHA channel) or layer information. Time-dependent spectral analysis of the burst can be performed only in those sections of the observation where there are no gaps in the GoodXenon data. However, we can construct a continuous light curve for the entire X-ray burst using Standard-1 data, which has no gaps.

For the spectral analysis of this burst, layer 1 events were extracted from the PCA FITS files for which unsaturated GoodXenon event data are available. We utilize version 5.3.1 of the HEASOFT FTOOLS package with XSPEC version 11.3.1 for the spectral fitting. This version of the FTOOLS generates response matrices with updated values of the default geometric areas for each PCU (Jahoda et al. 2005). These new effective areas improve the flux calibration of the Crab pulsar plus nebula so that the Crab flux is consistent with the standard value. This makes adjustments to the flux such as those utilized by Kuulkers et al. (2003) no longer necessary. Dead-time corrections are applied (always $<7.6\%$) to the observed count rates and spectra.

We fix the persistent X-ray emission for the source by extracting the spectrum of the 200 s of data before the X-ray burst began and use this as a fixed background for the burst spectral analysis. The Standard-1 mode light curve is shown in Figure 1. Examination of Figure 1 shows that this preburst segment of data has relatively little flickering or dipping behavior that might signify locally intervening material in the EXO 0748−676 system, and we therefore ignore this effect in our analysis. We fit the GoodXenon spectral data derived from segments of the burst profile to a model consisting of the XSPEC blackbody emission function multiplied by a photoelectric absorption function: `wabs×bbodyrad`. The interstellar hydrogen column density is frozen at 4.0×10^{21} cm^{-2} obtained by Thomas et al. (1997) from *ASCA* measurements. This allows the fitted parameters for the X-ray burst itself to vary independently of the persistent emission. For our spectral fits we include counts in the energy range 2.0–20 keV. We generate one response matrix for the entire X-ray burst observation that corresponds to approximately 100 s of time, and we assume zero systematic error in the fitting procedure. The resulting reduced χ^2 values for the spectral fits are all in the range 0.5–2.0. This procedure is similar to the analysis method of Smale (2001) for an X-ray burst observed from X2127+119 in the globular cluster M15. As a test of our method, we analyzed the *RXTE* archival data for the same X-ray burst observed by Smale (2001) and found results similar to his, which confirms that our analysis procedure is reliable.

3. BURST OSCILLATION SEARCH

The unusual strength of this burst makes it particularly attractive for burst oscillation searches. Villarreal & Strohmayer (2004) found evidence for a 45 Hz pulsation frequency in an incoherent sum of power spectra from 38 bursts from EXO 0748−676, but oscillations have never been detected in a single burst. We searched both the GoodXenon and burstcatcher data for coherent oscillations during this strong burst.

The burstcatcher data were binned at 122 μs intervals for 10 s starting about 1 s before the beginning of the burst. These data are continuous but have no energy resolution. The GoodXenon data have some gaps during the brightest part of the burst because the telemetry buffers filled. However, full energy resolution was available, and we searched 100 s of data beginning at 0.5 s before the burst. We created three time series to search for pulsations, one from the burstcatcher data with 122 μs bins and two from the GoodXenon data with 244 μs bins with energy selections of 2.5–6.0 keV and 6.0–60.0 keV. All three time series were searched for oscillations using the `powspec` FTOOL. A third-order polynomial was removed from each data window to reduce the red noise from the overall burst profile, and power spectra were Leahy-normalized. Several combinations of the fast Fourier transform window length (from 2048 to 32,768 points) and numbers of power spectra averaged (summing from 1 to 10 individual power spectra) were searched to maximize sensitivity to oscillations that occur with various timescales.

No oscillations were found during the X-ray burst. The precise upper limit on the oscillation amplitude depends on the assumed duration of the oscillations, but for averages of four 8192 point (2 s) intervals in the 6.0–60 keV time series, we would easily have detected sinusoidal pulsations whose rms was at least 5% of the total rms fluctuations. However, we would not have detected burst oscillations with an amplitude of only 3%, such as those found by Villarreal & Strohmayer (2004).

4. BURST SPECTRAL ANALYSIS

In our discussion of the burst physics we adopt the notation of Ebisuzaki et al. (1984) and define the observed "blackbody radius" $R_{\rm bb}$ with respect to the bolometric luminosity L and the observed color temperature T_c using

$$L = 4\pi R_{\rm bb}^2 \, \sigma T_c^4. \tag{1}$$

Solving for the blackbody radius yields

$$R_{\rm bb} = \left(\frac{L}{4\pi\sigma T_c^4} \right)^{1/2}. \tag{2}$$

In the Ebisuzaki et al. (1984) development, the color temperature observed at infinity T_c is the physical temperature of the radiating plasma at the "color radius" r_c, where thermalization of the radiation occurs via either free-free absorption or

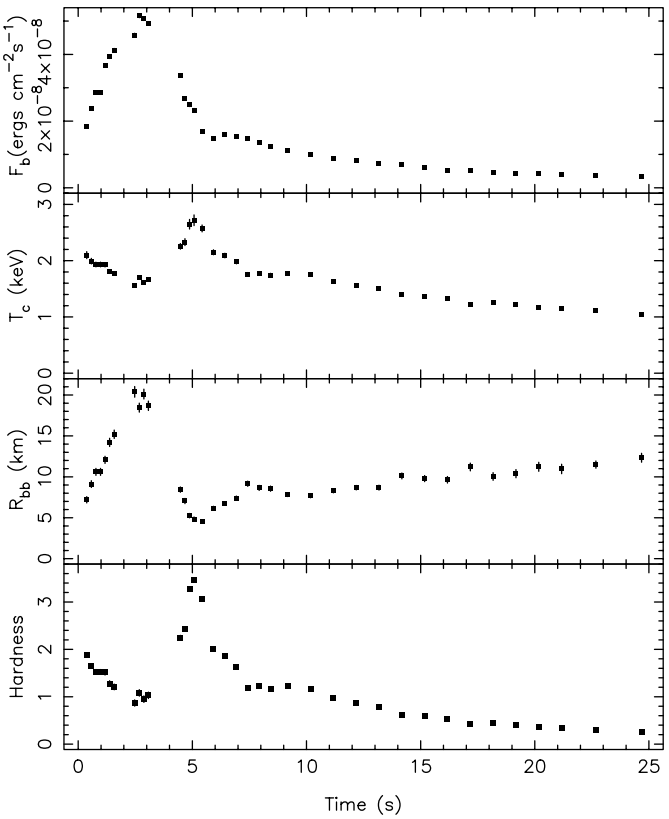

FIG. 2.—Results for the bolometric flux, observed color temperature, and blackbody radius from the spectral fit during the X-ray burst assuming a distance of 7.7 kpc. Note the gaps in the data points beginning at 1.6 and 3.1 s. These correspond to the saturation of the GoodXenon event mode. The peak bolometric flux is $F_{\rm peak} = 5.16 \times 10^{-8}$ ergs cm^{-2} s^{-1}.

Compton scattering. In this sense, the color radius can be interpreted as the standard photospheric radius. On the other hand, $R_{\rm bb}$ is not a true physical radius but rather a parameter that ensures that the observed spectral flux is correctly fitted in the `bbodyrad` model. Ebisuzaki et al. showed that $R_{\rm bb}$ is related to the color radius via $r_c = SR_{\rm bb}$, where $S = (3\tau_c/4)^{1/2}$ is the "radius expansion factor" and τ_c is the electron scattering optical depth to the color radius (see also London et al. 1986; Smale 2001). Physically, the distinction between the two radii arises as a consequence of electron scattering. The presence of a relatively deep scattering layer above the color radius reduces the diffusion velocity of the photons, which in turn reduces the outgoing flux. In order to carry the required luminosity, r_c must therefore exceed the value of $R_{\rm bb}$ computed using equation (2), since this expression completely ignores the effect of diffusion by implicitly assuming that the radiation is directly emitted from the "naked" stellar surface. Hence, $R_{\rm bb}$ is significantly smaller than the true physical radius r_c during the scattering-dominated, brightest part of the burst. This point is further discussed below.

The value of the Eddington luminosity $L_{\rm Edd}$ observed at infinity is given by the standard expression as modified by Lewin et al. (1993) and Galloway et al. (2003),

$$L_{\rm Edd} = \frac{4\pi G M_* c}{\kappa_{\rm sc}} \left(1 - \frac{2GM_*}{c^2 r_c}\right)^{1/2} \left[1 + (2.2 \times 10^{-9} T_c)^{0.86}\right], \quad (3)$$

where M_* is the neutron star mass (taken to be 1.4 $M_\odot$) and $\kappa_{\rm sc}$ is the electron scattering cross section. The temperature-dependent factor in brackets in equation (3) expresses the high-temperature modification of the scattering cross section. This set of general relativistically correct relations allows us to determine the distance to EXO 0748−676.

TABLE 1
EXO 0748−676 BURST AND DERIVED PARAMETERS

Parameter	Value
Burst fluence ($= E_b$) (ergs cm^{-2})	3.60×10^{-7}
Peak bolometric flux ($= F_{\rm peak}$) (ergs cm^{-2} s^{-1})	5.16×10^{-8}
Persistent flux ($= F_{\rm per}$) (ergs cm^{-2} s^{-1})	4.81×10^{-10}
γ $[= F_{\rm per}/(F_{\rm peak} - F_{\rm per})]$	0.0094
α $(= F_{\rm per}\Delta T/E_b)$[a]	17
τ $(= E_b/F_{\rm peak})$	7.0
Derived Parameters Assuming Hydrogen Burst Photosphere	
EXO 0748−676 distance from Sun[b,c] (kpc)	5.9 ± 0.9
EXO 0748−676 distance to Galactic center[b] (kpc)	9.5
EXO 0748−676 distance below Galactic plane (kpc)	2.0
Burst energy output (ergs)	1.48×10^{39}
Persistent accretion rate $\dot{M}_{\rm per}$ ($M_\odot$ yr^{-1})	1.68×10^{-10}
Derived Parameters Assuming Helium Burst Photosphere	
EXO 0748−676 distance from Sun[b,c] (kpc)	7.7 ± 0.9
EXO 0748−676 distance to Galactic center[b] (kpc)	10.5
EXO 0748−676 distance below Galactic plane (kpc)	2.6
Burst energy output (ergs)	2.54×10^{39}
Persistent accretion rate $\dot{M}_{\rm per}$ ($M_\odot$ yr^{-1})	2.89×10^{-10}

[a] Assuming a burst recurrence time of $\Delta T = 0.285$ hr (D. K. Galloway et al. 2005, in preparation).
[b] Assuming a solar system distance to the Galactic center of 8.5 kpc.
[c] Assuming $L_{\rm peak} = L_{\rm Edd}$.

The X-ray burst takes ~2.5 s to rise to its peak count rate in the light curve shown in Figure 2. This rise takes the observed flux from a persistent source-plus-background count rate of 276 counts s^{-1} in the 2–20 keV energy range (~16 mcrab) to a burst peak rate over 18,000 counts s^{-1}. The EXO 0748−676 orbital phase at the start of the burst is $\phi = 0.034220$ (4), roughly 230 s after eclipse egress. After this, the flux spends ~1.7 s within 90% of the peak count rate. The flux then falls rapidly for ~2 s down to a plateau at a level ~30% of the peak rate and then starts a rapid exponential decay with an *e*-folding time of 14 s. The principal parameters we derive for this burst are given in Table 1.

In Figure 2 the results of our spectral fitting are presented for the helium-rich photosphere case. The hardness ratio we plot is the ratio of the flux in the 6–20 keV energy band to the flux in the 3–6 keV energy band. When the observed flux reaches its peak, the apparent blackbody radius $R_{\rm bb}$ also reaches its maximum value as seen in Figure 2. As the observed blackbody radius initially expands to ~20 km, the observed color temperature decreases to a local minimum at the moment the radius achieves its largest value. In a similar fashion, the hardness ratio falls, reaching a local minimum as the observed flux is reaching its peak. The hardness ratio then dramatically increases again, reaching its maximum value ~2 s after the flux has begun to decay. The decrease in both the temperature and the hardness ratio while the flux is near its peak is indicative of the cooling that occurs during the photospheric expansion (Strohmayer & Bildsten 2005). After the flux reaches its peak and begins to decay, the radius drops rapidly to an apparent minimum of ~4.6 km and then recovers and asymptotically approaches ~13 km. As $R_{\rm bb}$ decreases after the peak, the temperature quickly rises to its largest values just as the flux is also decreasing. When the radius

reaches its minimum value, just after the peak of the burst, the temperature and the hardness ratio each reach their respective maxima. After this the burst begins its exponential decay until it fades away completely.

We derive an unabsorbed burst fluence of 3.60×10^{-7} ergs cm^{-2} by multiplying the unabsorbed flux in the energy range 2.0–20.0 keV by a bolometric correction and then integrating over the duration of the burst rise and decay. The bolometric correction is computed as a function of time by dividing the total blackbody flux by the blackbody flux in the 2.0–20.0 keV energy range based on the sequence of observed color temperatures. Assuming that the expanding envelope is helium-dominated, and that the peak flux of 5.16×10^{-8} ergs cm^{-2} s^{-1} corresponds to the Eddington luminosity of 3.64×10^{38} ergs s^{-1} for a 1.4 $M_\odot$ neutron star, we derive a distance of 7.67 kpc to EXO 0748−676. On the other hand, if the burst photosphere has solar abundances, then the peak flux corresponds to an Eddington luminosity of 2.12×10^{38} ergs s^{-1} for a 1.4 $M_\odot$ neutron star and a distance of 5.85 kpc to EXO 0748−676. The associated values of $L_{\rm Edd}$ for hydrogen- and helium-rich photospheres are consistent with the peak luminosities obtained by Kuulkers et al. (2003) in their analysis of photospheric radius expansion bursts in globular cluster sources, which have known distances. We note that the peak flux we obtain is ∼26% higher than the apparent peak flux obtained by Gottwald et al. (1986) for three photospheric radius expansion bursts from EXO 0748−676 observed by *EXOSAT*. Galloway et al. (2003) found that in photospheric radius expansion bursts from the LMXB 4U 1728−34 the peak fluxes were not constant but instead exhibited variations with a rms deviation of 9.4% and a total variation of 46%. Galloway et al. concluded that this variation might be caused by variable obscuration from a warped accretion disk around the neutron star. If the accretion disk surrounding the neutron star in EXO 0748−676 is also warped, then this could cause the same type of variations in peak fluxes as those observed in 4U 1728−34, which could explain why our peak flux is higher than that of Gottwald et al. (1986). If our higher flux is a result of less obscuration by a warped accretion disk, then the distance we derive will be more accurate than a distance based on the lower *EXOSAT* flux because our peak flux is more indicative of the unobscured Eddington flux for EXO 0748−676.

The EXO 0748−676 system is located at Galactic latitude $-19\overset{\circ}{.}8$ and Galactic longitude $280\overset{\circ}{.}0$. Hence, if we assume that the Galactic center is 8.5 kpc from the solar system, then EXO 0748−676 is ∼10.5 kpc from the Galactic center and ∼2.6 kpc below the Galactic plane. The ratio of the persistent X-ray flux from the preburst spectrum to the Eddington flux at the peak of the burst is $\gamma = 0.0094$ (see Table 1), which is consistent with the assumption that EXO 0748−676 is an atoll LMXB source. The distance implied by the helium-rich photosphere case combined with the observed persistent X-ray flux yields a mass accretion rate of $\sim 2.9 \times 10^{-10}\ M_\odot$ yr^{-1}, which is in the accretion rate range expected to yield mixed hydrogen and helium burning triggered by thermally unstable helium ignition (Strohmayer & Bildsten 2005). On the other hand, if the burst photosphere is hydrogen-rich, then the closer distance implies a lower persistent $\dot{M}$, pushing $\dot{M}$ into the range that results in burst ignition via thermally unstable hydrogen burning (Strohmayer & Bildsten 2005). Thus, conclusions about the characteristics of the burning for this X-ray burst depend on the assumed composition of the burst photosphere.

A number of possible sources of error exist for our estimated distance to EXO 0748−676. First, if the assumed mass of the neutron star ($M_* = 1.4\ M_\odot$) is incorrect, then the Eddington luminosity has been incorrectly calculated and the distance must be adjusted accordingly. For a 1.6 (1.2) $M_\odot$ neutron star we derive a distance of 8.2 (7.1) kpc from the same spectral fitting data for a helium-dominated burst. A second source of error enters through our estimate of the burst bolometric flux, either due to errors in the PCA calibration or errors in the bolometric corrections derived from the fitted temperatures. If the flux is 20% too high (low), we estimate that the source distance would change to 7.0 (8.6) kpc, again for a helium-dominated burst. The error estimates for the hydrogen-rich burst case are similar.

The increase in $R_{\rm bb}$ during the early phase of the burst clearly suggests that the photospheric radius of the radiating atmosphere expands. However, the subsequent minimum value of $R_{\rm bb} \sim 4.6$ km just after the burst peak is only about one-third of the apparent radius that a distant observer would associate with a 1.4 $M_\odot$ neutron star with a proper radius of 10 km, which is about 13 km when the gravitational redshift is included (Shapiro & Teukolsky 1983; Lattimer & Prakash 2001). If one expects a proper neutron star radius of ∼ 10 km, then that in turn suggests that the `bbodyrad` model in XSPEC does not include all of the physics involved in producing a radius expansion X-ray burst light curve. Without a clear understanding of the physics involved in the light-curve production after the peak of the burst, the derived radii cannot be reliably used to constrain either the neutron star radius or the equation of state of the nuclear matter (see the discussion of this point in Lewin et al. 1993). During the early, high-temperature portion of the burst around the time of the peak flux, the thermalization of the emitted radiation is almost certainly dominated by Comptonization. In this situation, the scattering depth to the color radius, τ_c, is related to the observed color temperature, T_c, via $\tau_c = (m_e c^2/4kT_c)^{1/2}$ (London et al. 1984, 1986; Smale 2001). On the basis of the observed color temperature at the peak of the burst, we find that $\tau_c \sim 5$, and therefore $S \sim 2$, where S is the radius expansion factor defined above. This implies that the color radius r_c is roughly double the blackbody radius just after the burst peak, when $R_{\rm bb}$ achieves its minimum value. However, even a factor of 2 increase in $R_{\rm bb}$ is not sufficient to bring the color radius r_c into accord with the apparent radius of 13 km. It should be noted that the canonical value of 10 km for the proper radius of the neutron star is based on a particular equation of state for the nuclear matter, and some alternative equations may allow slightly more compact neutron stars (Heiselberg & Pandharpande 2000), with proper radii perhaps as small as 9 km. However, this adjustment does not appear to be sufficient to completely remove the discrepancy cited above.

With regard to the post–peak-flux drop in $R_{\rm bb}$, it is possible that nonthermal spectral distortions could be created by ionized material located along the line of sight. Such material could rise from the accretion disk due to strong heating and photoionization driven by the peak X-ray flux. Preferential absorption of the soft radiation by the ionized gas would decrease the total flux while also causing the apparent color temperature to rise, in agreement with the observations (see Fig. 2). These two effects will cause a reduction in the value of $R_{\rm bb}$ computed using equation (2). In this sense, the X-ray burst will have created its own "weather" that it must shine through if the photons are to reach the PCA. There is some evidence for the existence of ionized gas in the vicinity of the binary system 4U 1820−303 during X-ray bursts, although no detailed model for this phenomenon has appeared (Strohmayer & Brown 2002). Presumably, after the early phase of strong irradiation, the ionized material drops back down into the disk, and therefore the differential absorption effect disappears. However, it is not clear whether

the dynamical and thermal timescales in the gas support this interpretation.

5. CONCLUSIONS

We have analyzed an unusually strong X-ray burst from the LMXB EXO 0748−676 and found that it shows evidence for photospheric radius expansion. No oscillations were detected during the X-ray burst despite an exhaustive search. When we equate the peak flux from the X-ray burst with the expected Eddington flux from a 1.4 $M_{\odot}$ neutron star, we derive a distance to the EXO 0748−676 system of 7.7 kpc for a helium-dominated burst photosphere and 5.9 kpc for a hydrogen-dominated burst photosphere. While we have argued that our distance determination to EXO 0748−676 is likely to be more accurate than previous determinations, the ambiguity in the distance determinations between hydrogen- and helium-rich photospheric abundances in the real Eddington luminosity remains. Thus, we must quote a range of distances accounting for both abundance cases. Only when the observational characterizations of burst properties are able to fix the abundances of the bursting neutron star photosphere can this ambiguity in distance determinations to bursting LMXB systems be overcome. The X-ray burst flux light curve strongly suggests that we do not completely understand the physics of the spectral formation process in an X-ray burst just after maximum brightness, when the luminosity is beginning to recede from the Eddington limit. If the derived distance is correct, then the small values obtained for the fitted blackbody radius $R_{\rm bb}$ after the peak of the burst are difficult to reconcile with the 10 km proper radius of the star, even when adjustments are made using the high electron scattering optical depth. Possible alternative explanations include the presence of intervening material that absorbs the soft flux after the peak or perhaps the occurrence of nonspherical mass motions.

We are pleased to acknowledge discussions with Craig Markwardt, Jean Swank, Deepto Chakrabarty, Duncan Galloway, Jeroen Homan, and Lev Titarchuk. This research is supported by the Office of Naval Research, the NASA Astrophysical Data Program, and the NASA *RXTE* Guest Observer Program.

REFERENCES

Cottam, J., Paerels, F., & Mendez, M. 2002, Nature, 420, 51
Crampton, D., Cowley, A. P., Stauffer, J., Ianna, P., & Hutchings, J. B. 1986, ApJ, 306, 599
Ebisuzaki, T., Hanawa, T., & Sugimoto, D. 1984, PASJ, 36, 551
Galloway, D. K., Psaltis, D., Chakrabarty, D., & Muno, M. P. 2003, ApJ, 590, 999
Gottwald, M., Haberl, F., Parmar, A. N., & White, N. E. 1986, ApJ, 308, 213
Heiselberg, H., & Pandharpande, V. 2000, Ann. Rev. Nucl. Part. Sci., 50, 481
Hertz, P., Wood, K. S., & Cominsky, L. R. 1997, ApJ, 486, 1000
Jahoda, K., Markwardt, C. B., Radeva, Y., Rots, A. H., Stark, M. J., Swank, J. H., Strohmayer, T. E., & Zhang, W. 2005, ApJS, submitted
Jonker, P. G., & Nelemans, G. 2004, MNRAS, 354, 355
Kuulkers, E., den Hartog, P. R., in't Zand, J. J. M., Verbunt, F. W. M., Harris, W. E., & Cocchi, M. 2003, A&A, 399, 663
Lattimer, J. M., & Prakash, M. 2001, ApJ, 550, 426
Lewin, W. H. G., van Paradijs, J., & Taam, R. E. 1993, Space Sci. Rev., 62, 223
London, R. A., Taam, R. E., & Howard, W. M. 1984, ApJ, 287, L27
———. 1986, ApJ, 306, 170
Parmar, A. N., White, N. E., Giommi, P., & Haberl, F. 1985, IAU Circ., 4039, 1
Schoembs, R., & Zoeschinger, G. 1990, A&A, 227, 105
Shapiro, S. L., & Teukolsky, S. A. 1983, Black Holes, White Dwarfs, and Neutron Stars: The Physics of Compact Objects (New York: Wiley)
Smale, A. P. 2001, ApJ, 562, 957
Strohmayer, T., & Bildsten, L. 2005, in Compact Stellar X-Ray Sources, ed. W. H. G. Lewin & M. van der Klis (Cambridge: Cambridge Univ. Press), in press (astro-ph/0301544)
Strohmayer, T. E., & Brown, E. F. 2002, ApJ, 566, 1045
Thomas, B., Corbet, R., Smale, A. P., Asai, K., & Dotani, T. 1997, ApJ, 480, L21
van Paradijs, J., van der Klis, M., & Pedersen, H. 1988, A&AS, 76, 185
Villarreal, A. R., & Strohmayer, T. E. 2004, ApJ, 614, L121
Wade, R. A., Quintana, H., Horne, K., & Marsh, T. R. 1985, PASP, 97, 1092
Wolff, M. T., Hertz, P., Wood, K. S., Ray, P. S., & Bandyopadhyay, R. M. 2002, ApJ, 575, 384